PCCP

PAPER

View Article Online
View Journal | View Issue

Cite this: *Phys. Chem. Chem. Phys.*, 2025, **27**, 17063

A thermodynamic assessment of the decomposition and rehydrogenation of o1-$Ba(BH_4)_2$ based on DFT calculations and correlation functions

Konrad Burkmann, [a] Markus Mehlhorn, [ab] Angus Demmer,[a] Jakob Kraus, [b] Franziska Habermann, [a] Jürgen Seidel,[a] Klaus Bohmhammel,[a] Jens Kortus [b] and Florian Mertens *[ac]

Received 25th February 2025,
Accepted 18th July 2025

DOI: 10.1039/d5cp00744e

rsc.li/pccp

In this study, an estimate is given for the enthalpy of formation at 298.15 K for the room temperature phase of barium boranate, o1-$Ba(BH_4)_2$, based on correlations between well known enthalpies of formation of boranates and the corresponding values of the respective metal perchlorates and bromides as well as the Pauling electronegativity. A new procedure for estimating the absolute entropy at 298.15 K using metal bromides is presented as well. To evaluate this method, the absolute entropy value at 298.15 K was calculated from the Gibbs free energy function of o1-$Ba(BH_4)_2$. The Gibbs free energy function and corresponding heat capacity values between 5 K and 700 K were calculated applying density functional theory (DFT) and statistical thermodynamics using the quasi-harmonic approach. Furthermore, several thermodynamic calculations regarding possible synthesis reactions and decomposition routes of o1-$Ba(BH_4)_2$ are discussed.

Introduction

Metal hydrides and derivates are still in the focus of the research interests of the metal hydride community,[1–16] including not only high entropy alloys,[7,14] but also complex metal hydrides such as boranates[1–4,6,8–11,13,14] and alanates[1,5,10,14] as well as their derivates.[2,4,10,17–20] In recent years some investigations focussed on the determination of thermodynamic quantities of complex hydrides and based on that the thermodynamic modelling of their decomposition behaviour and rehydrogenation potential.[1,10,13,21–30] The main goal in this context is the design of a thermodynamically tuned system which can be used for reversible hydrogen storage under improved conditions for various applications, as it was shown in principle for $LiBH_4$ and MgH_2 by Vajo *et al.*[31,32]

$Ba(BH_4)_2$ was first synthesised and characterised by Wiberg *et al.*[33–35] in the 1950ies, together with $Ca(BH_4)_2$ and $Sr(BH_4)_2$ starting from different metal sources and gaseous diborane, as was explained elsewhere.[24,26] Some other reports dealed with the synthesis applying reactions between BaH_2 and BH_3-solvent adducts.[3,36] Mikheeva *et al.*[37] synthesised the compound by a metathesis reaction between $LiBH_4$ and BaI_2 in tetrahydrofurane (THF; see reaction eqn (1)) mentioning problems to achieve acceptable purity caused by remaining traces of LiI presumable found in the product as a consequence of its high solubility in THF.[38]

$$2LiBH_4 + BaI_2 \rightarrow 2LiI + Ba(BH_4)_2 \quad (1)$$

A very poor solubility of $Ba(BH_4)_2$ in THF is reported,[37,39] which can be improved by adding $LiBH_4$ to the solution.[39] The compound crystallises in four different modifications depending on the temperature, as indicated by Sharma *et al.*[36] Its decomposition behaviour was addressed in several studies[33,36,37] leading to two proposals for the decomposition scheme, either after reaction eqn (2)[33] or reaction eqn (3).[36]

$$Ba(BH_4)_2 \rightarrow BaH_2 + 2B + 3H_2 \quad (2)$$

$$Ba(BH_4)_2 \rightarrow \frac{2}{3}BaH_2 + \frac{1}{3}BaB_6 + \frac{10}{3}H_2 \quad (3)$$

The decomposition process starts with melting at about 385 °C[37] followed by the actual decomposition at temperatures higher than 400 °C[33] or even 500 °C.[8,36,37,40] This polymorph is stable up to 668 K, where it transforms into o2-$Ba(BH_4)_2$.[36]

[a] *Insitut für Physikalische Chemie, TU Bergakademie Freiberg, Lessingstraße 45, 09599 Freiberg, Germany. E-mail: Florian.Mertens@chemie.tu-freiberg.de; Fax: +49 3731 39-3588; Tel: +49 3731 39-3737*
[b] *Insitut für Theoretische Physik, TU Bergakademie Freiberg, Leipziger Straße 23, 09599 Freiberg, Germany*
[c] *Zentrum für Effiziente Hochtemperatur-Stoffwandlung, TU Bergakademie Freiberg, Winklerstraße 5, 09599 Freiberg, Germany*

Unfortunately, we were not able to produce a high-purity sample of $Ba(BH_4)_2$ using the well established method of metathesis reactions,[41] which was demonstrated to be successful by our group in many other cases for complex metal hydrides (*e.g.* ref. 23–26 and 28–30) to perform our own investigations. Therefore, we decided to conduct a theoretical study using DFT calculations, statistical thermodynamics and some thermodynamic estimates regarding the room temperature phase of barium boranate, o1-$Ba(BH_4)_2$. With these data we investigated the decomposition behaviour and rehydrogenation potential of the decomposition products by thermodynamic calculations and compared the results with experimental data.

Methods to determine thermodynamic data and respective calculations

Computation

Density functional theory (DFT) was used to calculate thermodynamic state functions of $Ba(BH_4)_2$.[42] All computations were carried out using the plane-wave program Quantum ESPRESSO version 7.3.[43–45] The generalized gradient exchange–correlation functional PBEsol[46] in combination with pseudo potentials from the standard solid-state pseudopotentials (SSSP) PBEsol precision library[47] was applied for the electronic structure calculations. For the statistical thermodynamical calculations based on the quantum mechanical results the python package pwtools by Steve Schmerler was used.[48]

Thermodynamic data from correlation functions

There exist several possibilities to estimate the values of thermodynamic quantities of complex hydrides. The most common method exploits the correlation between the electronegativity of the metal and the enthalpy of formation of the respective metal boranate,[1,14,49,50] which was introduced by Nakamori *et al.*[49] In addition, there are a couple of reports focussing on the estimation of enthalpy of formation values of metal boranates by correlating them with the respective ones of metal perchlorates,[51] metal alanates,[28,52,53] metal bromides[54] or other quantities.[52] Additionally, some of the literature reports on the estimation of absolute entropy values of complex metal hydrides from the correlation with data from the corresponding metal perchlorates[28,53] as well as with other (complex) metal hydrides.[28,52,53]

Furthermore, there is the possibility to estimate the absolute entropy of a given compound by integrating the heat capacity function applying the Neumann–Kopp rule.[53] For this purpose, the modified Neumann–Kopp procedure presented by Pinatel *et al.*[22] can be used, which assumes the contribution of the "BH_4"-part of the boranate in question to the total heat capacity as being equal to the difference of the heat capacities of $NaBH_4$ and metallic sodium. As it is the case for the Neumann–Kopp rule based solely on the elements, the contribution of the metal contained in the metal boranate investigated (in our case Ba) is reflected by the heat capacity of the metal in elemental form. However, Dematteis *et al.*[21] showed that this method delivers only rough estimates of the C_P function. Our group found the same limitation for $Y(BH_4)_3$ using $LiBH_4$ and Li for the estimate of the BH_4 contribution.[24] Given these discrepancies, we will not apply this method here, as there are large errors between the absolute entropy at 298.15 K estimated using these Neumann–Kopp heat capacity values and the experimental determined one.[24]

In this study we will show correlations between the enthalpies of formation as well as the absolute entropies of selected metal perchlorates, metal bromides and the respective metal boranates. The correlation between the Pauling electronegativity and the enthalpy of formation will be also be presented. The correlations between the thermodynamic quantities of metal boranates and the corresponding metal alanates to estimate these values are not taken into account, because there are only few thermodynamic values available from the literature for metal alanates (*e.g.* ref. 28–30, 53 and 55). All necessary data for the applied correlations are given in Tables 1 and 2.

Table 1 Input data for the estimation of the enthalpy of formation of $Ba(BH_4)_2$ at 298.15 K, taken from HSC 5.1 data base,[55] if not indexed further, whereby χ_P denotes the Pauling electronegativity, taken from ref. 56

			$\Delta_F H$(298.15 K) (kJ mol^{-1})			
M	n	χ_P	$M(BH_4)_n$	$M(ClO_4)_n$	MBr_n	Commentary
Li	1	0.98	−190.464	−380.744	−351.160	
Na	1	0.93	−188.698	−382.752	−361.160	
K	1	0.82	−226.898	−432.751	−393.450	
Rb	1	0.82		−394.770	−434.592	
Cs	1	0.79		−437.228	−405.600	
Mg	2	1.31	−104.5[22]	−293.500	−262.150	
Ca	2	1	−183.079[57]	−362.500	−341.900	β-$Ca(BH_4)_2$
Sr	2	0.95		−370.285	−358.987	
Ba	2	0.89		−398.130	−378.650	
Y	3	1.22	−124.1 ± 1.5[58]		−286.0 ± 0.7[59]	α-$Y(BH_4)_3$
La	3	1.1	−151.6 ± 0.1[60]		−302.364	
Zr	4	1.33	−65.2[23]		−190.175	
Hf	4	1.3	−57.0[23]		−191.575	

Table 2 Input data for the estimation of the absolute entropy of $Ba(BH_4)_2$ at 298.15 K, taken from HSC 5.1 data base,[55] if not indexed further

		S(298.15 K) (J mol^{-1} K^{-1})			
M	n	$M(BH_4)_n$	$M(ClO_4)_n$	MBr_n	Commentary
Li	1	75.818	125.520	74.010	
Na	1	101.391	142.256	86.930	
K	1	106.608	151.042	95.920	
Rb	1	126.6[61]	160.666	110.100	
Cs	1	141.8[61]	175.268	112.940	
Mg	2	65.78[22]	109.000	58.500	
Ca	2	58.7 ± 2.1[24]	116.525	65.000	β-$Ca(BH_4)_2$
Sr	2	73.6 ± 2.2[26]	123.847	71.756	
Ba	2		120.709	75.000	
Y	3	56.3 ± 1.7[25]		63.6[62]	α-$Y(BH_4)_3$
La	3			59.2733	
Zr	4	57.1[23]		56.175	
Hf	4	53.2[23]		59.622	

Thermodynamic equilibrium calculations

The thermodynamic equilibrium calculations were carried out using the Software HSC 5.1[55] and the data for all relevant

Table 3 Thermodynamic data of compounds involved in the thermodynamic equilibrium calculations – data taken from HSC 5.1,[55] if not indexed further

Compound	$\Delta_F H^\circ$(298.15 K) (kJ mol^{-1})	S°(298.15 K) (J mol^{-1} K^{-1})	T (K)	Coefficients of the heat capacity function a	b	c	d
$H_{2(g)}$	0	130.679	298.15–5000	25.855	4.837	1.584	−0.372
B	0	5.900	298.15–1500	16.033	12.895	−7.570	−3.234
BaH_2	−190.079	62.998	298.15–871	38.585	25.234	−0.268	2.138
BaB_6[64]	−281.619	96.704	298.15–1000	110.470	86.037	−58.619	−22.279
$BaBr_2$	−757.300	150.000	100–1130	70.117	21.992	−0.650	0.000
$BaCl_2$	−855.200	123.666	298.15–1198	90.228	−33.895	−7.213	34.388
BaF_2	−1208.758	96.399	298.15–900	90.228	−35.677	−9.682	39.062
BaI_2	−605.425	165.142	298.15–984	70.927	21 606	0.201	−1.117
$LiBH_4$	−190.464	75.818	298.15–400	−46.710	677.929	1.728	−840.871
LiBr	−351.160	74.010	298.15–823	40.704	26.059	1.206	−0.004
LiCl	−408.266	59.300	298.15–883	44.707	17.924	−1.946	1.865
LiF	−616.931	35.660	298.15–700	50.317	−2.492	−7.991	13.838
LiI	−270.412	86.710	298.15–742	43.630	24.848	0.002	−0.011
$NaBH_4$	−188.698	101.391	298.15–400	32.409	274.278	−1.682	−290.759
NaBr	−361.160	86.930	298.15–1020	43.839	20.302	1.323	−0.005
NaCl	−411.120	72.132	298.15–1074	47.100	7.220	0.209	11.200
NaF	−576.600	51.212	100–1269	46.717	6.912	−2.485	6.466
NaI	−287.817	98.560	298.15–934	41.967	25.190	2.322	−0.001

compounds are listed in Table 3. The heat capacity functions were used in the form of the well-established Maier–Kelley polynom[63] (see eqn (4)).

$$\frac{C_P}{[\mathrm{J\ mol^{-1}\ K^{-1}}]} = a + b\cdot\frac{T}{[\mathrm{K}]}\cdot 10^{-3} + c\cdot\frac{T^{-2}}{[\mathrm{K^{-2}}]}\cdot 10^{5} + d\cdot\frac{T^{2}}{[\mathrm{K^{2}}]}\cdot 10^{-6} \quad (4)$$

Results

DFT and statistical thermodynamics

The heat capacity function of $Ba(BH_4)_2$ was calculated from electronic energies and phononic densities of state (DOS) using DFT under the condition of the quasi-harmonic approximation. This approach was already successfully applied to $Zr(BH_4)_4$ and $Hf(BH_4)_4$[23] and several alanates.[29,30]

The starting geometry for the following computations is orthorhombic barium borante (o1-$Ba(BH_4)_2$)[36] at room temperature, whereby the CIF was taken from the ICSD[65] (collection code: 252859). Convergence tests were applied to this structure using the PBEsol functional and SSSP pseudopotentials. The kinetic energy cutoff of the wavefunction (ECUTWFC) was increased in steps of 10 Ry and subsequently the kinetic energy cutoff of the density (ECUTRHO) was varied in integer multiples of ECUTWFC. Additionally, $n \times n \times n$ Monkhorst–Pack k-grids of different tightness were tested. These parameters were successively increased until the electronic energy changed less than 10^{-3} meV atom^{-1}. To guarantee a sufficiently converged density for following density functional perturbation theory (DFPT) calculations, ECUTRHO was chosen twice as high as the necessary value obtained from the convergence test. Consequently, an ECUTWFC of 100 Ry, an ECUTRHO of 800 Ry and a $4 \times 4 \times 4$ Monkhorst–Pack k-grid were applied for the following calculations.

Using the BFGS algorithm, the starting geometry was optimized under convergence thresholds of 10^{-3} Ha a_0^{-1} for force, of 10^{-3} Ha for energy and 0.1 kbar for the pressure of the unit cell. The volume of this PBEsol optimized geometry was then scaled in a range from 95.5% to 114.5%. The generated volumes were geometry optimized again under constant volume. Respective dynamical matricies were computed using DFPT[66–68] on a $2 \times 2 \times 2$ wave vector grid. After Fourier transform of the dynamical matrix to real space one obtains the force constants. The phononic DOS was determined on a $10 \times 10 \times 10$ wave vector grid. An example for a cell with 223.1 Å^3 volume is given in Fig. 1.

A comparison with the DOS of other boranates[49,50,69–71] shows a similar distribution of the states. In detail, there are three regions with the harmonic low-energy phonons at wave numbers lower than 500 cm^{-1} corresponding to accustic

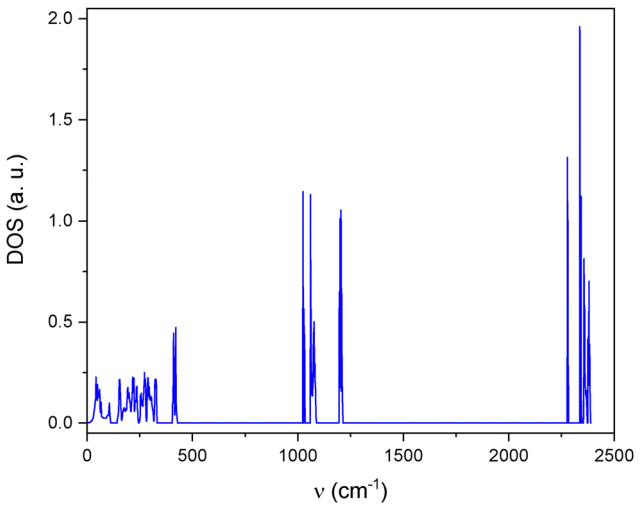

Fig. 1 Phononic DOS of $Ba(BH_4)_2$ at unit cell volume of 223.1 Å^3, which is the calculated unit cell closest to the room temperature volume.

phonons, which represent the librational modes of the Ba cations and "BH_4" anions, as explained by Miwa *et al.*[69] for $Ca(BH_4)_2$. The modes at higher frequencies correspond to B–H bending (about 1000 cm^{-1}–1300 cm^{-1}) and B–H stretching (about 2250 cm^{-1}–2400 cm^{-1}), respectively, as found for $Ca(BH_4)_2$[69] as well as $Y(BH_4)_3$.[71] Furthermore, Miwa *et al.*[69] found a good agreement with the Raman spectroscopy results of $Ca(BH_4)_2$.

Another feature can be extracted from an comparison with the DOS of metal alanates in the case of $Ca(AlH_4)_2$ reported by Wolverton and Ozolinš:[72] their stretching modes exhibit lower frequencies (and therefore energies) than the respective ones of boranates indicating lower thermal stabilities of alanates compared to boranates.[1,5,8,14,28,58] Therefore, it seems possible to use the phononic DOS of a certain compound to derive statements on the stability of this compound in comparison to compounds with comparable structures and properties.

The Gibbs free energy G was calculated for every volume as a function of the temperature based on the phononic DOS for a pressure of 1 bar. Subsequently, it was optimized in respect to the volume obtaining a function $G(T)$.[42,73] From a fit of the $G(T)$ function after dividing the temperature range in typical intervals, the fit coefficients corresponding to eqn (5) were extracted (see Table 4).

$$\frac{G(T)}{[\mathrm{J\ mol^{-1}}]} = A + B\cdot\frac{T}{[\mathrm{K}]} + C\cdot\frac{T}{[\mathrm{K}]}\cdot\ln\left(\frac{T}{[\mathrm{K}]}\right) + D\cdot\frac{T^2}{[\mathrm{K^2}]} + E\cdot\frac{T^3}{[\mathrm{K^3}]} + F\cdot\frac{T^{-1}}{[\mathrm{K^{-1}}]} + G\cdot\frac{T^4}{[\mathrm{K^4}]} + H\cdot\ln\left(\frac{T}{[\mathrm{K}]}\right) + I\cdot\frac{T^6}{[\mathrm{K^6}]} \quad (5)$$

Applying the negative derivative by the temperature of these $G(T)$ functions using eqn (6), the absolute entropy function $S(T)$ was obtained possessing a value of $S(298.15\ \mathrm{K}) = 144.3\ \mathrm{J\ mol^{-1}\ K^{-1}}$ at 298.15 K. To calculate the heat capacity function $C_P(T)$, the entropy function was differentiated and multiplied by the temperature according to eqn (7).

$$S(T) = -\left(\frac{\partial G(T)}{\partial T}\right) \quad (6)$$

Table 5 Calcualted coefficients of the heat capacity function of $Ba(BH_4)_2$ derived by applying eqn (9)–(15) to the coefficents of of ist $G(T)$ function from Table 4

T (K)	5–15	15–60	60–255	255–700
a	0	$-3.110\cdot10^{0}$	$-6.725\cdot10^{1}$	$5.644\cdot10^{1}$
b	0	$5.374\cdot10^{-1}$	$1.598\cdot10^{0}$	$2.690\cdot10^{-1}$
c	0	$6.482\cdot10^{-4}$	$-5.451\cdot10^{-3}$	$-1.095\cdot10^{-4}$
d	0	0	$1.708\cdot10^{3}$	$-2.564\cdot10^{5}$
e	$1.452\cdot10^{-3}$	0	$7.442\cdot10^{-6}$	0
f	0	0	$1.197\cdot10^{3}$	0
g	$-4.254\cdot10^{-7}$	0	0	0

$$C_P(T) = T\cdot\left(\frac{\partial S(T)}{\partial T}\right) \quad (7)$$

The coefficients of the derived heat capacity function according to eqn (8) are listed in Table 5. They can be derived using the known correlations between them and the coefficients of the $G(T)$ function,[74] as given in the eqn (9)–(15).

$$\frac{C_P}{[\mathrm{J\ mol^{-1}\ K^{-1}}]} = a + b\cdot\frac{T}{[\mathrm{K}]} + c\cdot\frac{T^2}{[\mathrm{K^2}]} + d\cdot\frac{T^{-2}}{[\mathrm{K^{-2}}]} + e\cdot\frac{T^3}{[\mathrm{K^3}]} + f\cdot\frac{T^{-1}}{[\mathrm{K^{-1}}]} + g\cdot\frac{T^5}{[\mathrm{K^{-5}}]} \quad (8)$$

$$a = -C \quad (9)$$

$$b = -2\cdot D \quad (10)$$

$$c = -6\cdot E \quad (11)$$

$$d = -2\cdot F \quad (12)$$

$$e = -12\cdot G \quad (13)$$

$$f = H \quad (14)$$

$$g = -30\cdot I \quad (15)$$

The graph displaying the calculated heat capacity values applying the coefficients from Table 5 is shown in Fig. 2. One can derive similar C_P values applying a numerical derivation using eqn (7) and (8), which is normally used to obtain C_P

Table 4 Coefficients of the determined $G(T)$ functions of $Ba(BH_4)_2$ including the fit quality parameters R^2 (coefficient of determination) and FitStdErr (fit standard error)

T [K]	5–15	15–60	60–255	255–700
A	$-1.025\cdot10^{8}$	$-1.025\cdot10^{8}$	$-1.025\cdot10^{8}$	$-1.025\cdot10^{8}$
B	0	$-5.151\cdot10^{0}$	$-2.988\cdot10^{2}$	$3.105\cdot10^{2}$
C	0	$3.110\cdot10^{0}$	$6.725\cdot10^{1}$	$-5.644\cdot10^{1}$
D	0	$-2.687\cdot10^{-1}$	$-7.991\cdot10^{-1}$	$-1.345\cdot10^{-1}$
E	0	$-1.080\cdot10^{-4}$	$9.085\cdot10^{-4}$	$1.825\cdot10^{-5}$
F	0	0	$-8.539\cdot10^{2}$	$1.282\cdot10^{5}$
G	$-1.210\cdot10^{-4}$	0	$-6.201\cdot10^{-7}$	0
H	0	0	$1.197\cdot10^{3}$	0
I	$1.418\cdot10^{-8}$	0	0	0
R^2	0.9998	1.000	1.000	1.000
FitStdErr [J mol^{-1}]	$7.086\cdot10^{-2}$	$1.487\cdot10^{-1}$	$1.995\cdot10^{-1}$	$9.841\cdot10^{-2}$

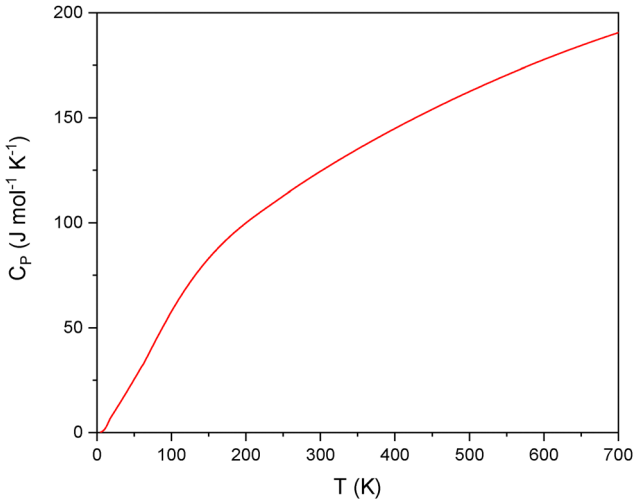

Fig. 2 Derived C_P values of $Ba(BH_4)_2$ using the coefficients from Table 5.

values derived from computations.[42] However, the C_P values obtained in this way fluctuate around the actual value at high temperatures, which led us to use the procedure described above.

The shape of the curve and the values derived are compatible with those of the other alkaline earth metal boranates.[23,24] Therefore, the results of the performed calculations appear to be trustworthy.

Estimation procedures

The literature data in Tables 1 and 2 were used to derive the values of thermodynamic quantities of $Ba(BH_4)_2$ by employing correlation procedures. The results of these procedures are shown in the following diagrams for which the corresponding fit coefficients and fit quality parameters can be found in Table 6. Using these coefficients one can derive estimates for the so far experimentally not explored boranates, like $Ba(BH_4)_2$.

Enthalpy of formation

Fig. 3 displays the correlation between the Pauling electronegativity and the enthalpy of formation of metal boranates. It has to be mentioned, that the values of the enthalpy of formation values of $Zr(BH_4)_4$ and $Hf(BH_4)_4$ were not used for the fit, as there is a large deviation from the expected linear behaviour. An similar deviation was found between their decomposition temperatures and the Pauling electronegativity and was explained by the molecular structure of both boranates compared to the more salt-like other boranates.[14] In contrast to these boranates, $Zr(BH_4)_4$ and $Hf(BH_4)_4$ are known to show a significant degree of covalent bonding.[23] It is noteworthy that the correlation function should be constructed only with boranates that are similar in respect to bonding to the boranate for which the enthalpy of formation is supposed to be estimated.

In Fig. 4 and 5 one can see that a linear direct correlation holds between the enthalpies of formation of boranates and of the bromides and perchlorates. The advantage of both the bromide and the perchlorate correlation is that the binding character between anion and cation is not an exclusion criterion for the inclusion of a boranate in the correlation, provided that both the boranate itself and the corresponding bromide or perchlorate have the same bonding character between anion and cation. However, in order to establish a correlation with the perchlorates one faces the problem of a lack of thermodynamic data.

The comparison of the obtained values for the enthalpy of formation of $Ba(BH_4)_2$ derived from the different methods applied shows a good agreement. Nevertheless, a significant uncertainty in the perchlorate case (about 10%) compared to those of the bromide (about 7%) and electronegativity (about 5%) ones was observed. For subsequent calculations the mean of all estimations from the different procedures tested will be used ((-413.0 ± 7.3) kJ mol^{-1}). The uncertainty of about 2% results from the two standard errors of the three estimated enthalpy of formation values and effects further thermodynamic calculations and is therefore taken into account later.

However, for $Y(BH_4)_3$, $La(BH_4)_3$, $Zr(BH_4)_4$ and $Hf(BH_4)_4$ the perchlorate correlation is not applicable, because no values of the enthalpies of formation of the respective perchlorates are available in the literature. Additionally, the use of the correlation function based on the Pauling electronegativity for $Zr(BH_4)_4$ and $Hf(BH_4)_4$ seems problematic, as pointed out due to the binding situation. These facts underline the greater applicability and reliability of the bromide correlation procedure.

Table 6 Fit coefficients with their standard errors for the shown correlation functions as well as calculated values for the enthalpy of formation and absolute entropy for $Ba(BH_4)_2$ – given uncertainties of the estimated values are derived using the 90% confidence limit of the fits and the uncertainties of the mean values are the two standard errors of the estimates[75,76]

		Fit coefficients		
Quantity	Correlation	*A*	*B*	Estimated values
$\Delta_F H$(298.15 K) (kJ mol^{-1})	$M(ClO_4)_n$	$(1.478 \pm 0.320) \cdot 10^2$	$(8.813 \pm 0.858) \cdot 10^{-1}$	-406.2 ± 42.6
	MBr_n	$(9.871 \pm 1.121) \cdot 10^1$	$(8.134 \pm 0.367) \cdot 10^{-1}$	-418.6 ± 29.5
	χ_P	$(-4.282 \pm 0.133) \cdot 10^2$	$(2.484 \pm 0.125) \cdot 10^2$	-414.3 ± 22.8
	Mean	—	—	-413.0 ± 7.3
S(298.15 K) (J mol^{-1} K^{-1})	$M(ClO_4)_n$	$(-8.325 \pm 1.261) \cdot 10^1$	1.283 ± 0.090	143.2 ± 19.5
	MBr_n	$(-3.072 \pm 0.745) \cdot 10^1$	1.468 ± 0.093	158.8 ± 13.6
	Mean	—	—	151.0 ± 15.6

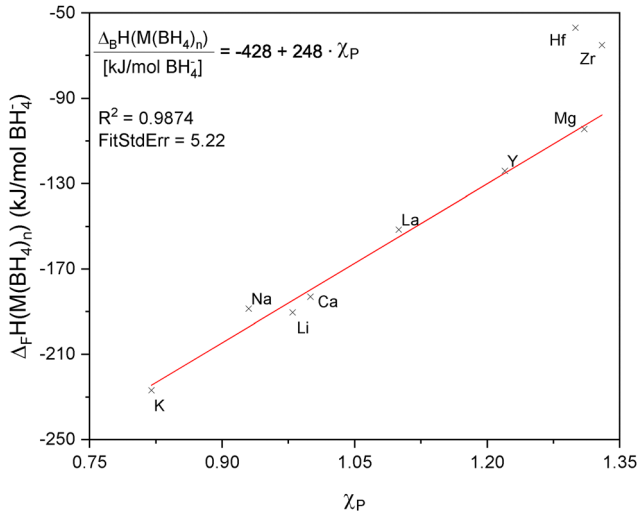

Fig. 3 Linear correlation between the enthalpies of formation of metal boranates and the Pauling electronegativity. The fit coefficients and the standard fit error corresponding to the linear fit function can be found in the diagram as well as in Table 6. The values of $Zr(BH_4)_4$ and $Hf(BH_4)_4$ were not used for determining the correlation function (explanation see text).

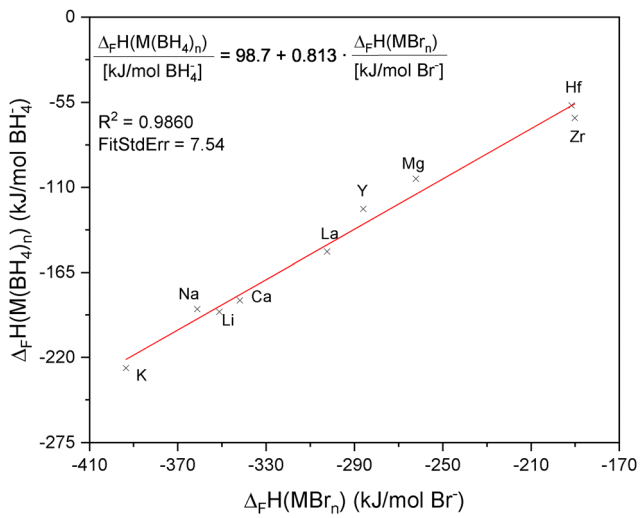

Fig. 4 Linear correlation between the enthalpies of formation of metal boranates and the ones of the corresponding metal bromides. The fit coefficients and the standard fit error corresponding to the linear fit function can be found in the diagram as well as in Table 6.

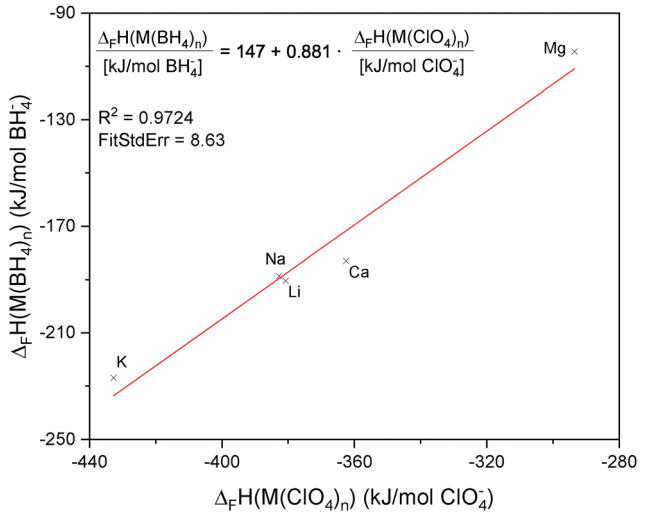

Fig. 5 Linear correlation between the enthalpies of formation of metal boranates and the ones of the corresponding metal perchlorates. The fit coefficients and the standard fit error corresponding to the linear fit function can be found in the diagram as well as in Table 6.

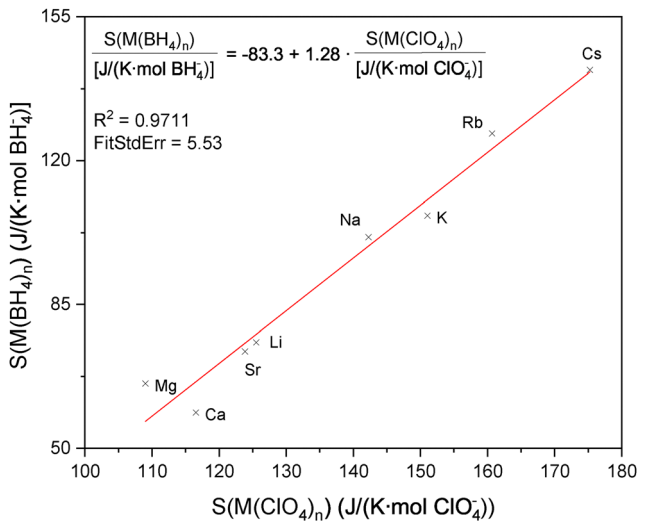

Fig. 6 Linear correlation between the absolute entropies of metal boranates and the ones of the corresponding metal perchlorates. The fit coefficients and the standard fit error corresponding to the linear fit function can be found in the diagram as well as in Table 6.

Absolute entropy

The plots for the estimation of the absolute entropies based on the mentioned correlation functions are given in Fig. 6 and 7. There are the same restrictions regarding the availability of data for metal perchlorates as in the case already described for their enthalpy of formation (*vide supra*).

The uncertainty of the absolute entropy value derived from the perchlorate correlation is slightly higher (about 14%) than that from the bromide correlation (about 9%). Combining both absolute entropy values and their uncertainties derived by the shown procedures,[75,76] results in the value of (151.0 ± 15.6) J mol^{-1} K^{-1} for the absolute entropy of $Ba(BH_4)_2$. Fortunately, we can compare this value with the DFT calculated one (*vide supra*), of 144.3 J mol^{-1} K^{-1}. Taking into account the uncertainty of the estimated value, the DFT value seems reasonable and is used within all further calculations below.

Thermodynamic synthesis analysis

As already mentioned, our group was not able to synthesise $Ba(BH_4)_2$ by using metathesis reactions.[41,58] Furthermore, there is only one report regarding a wet chemical route.[37] This section will give an overview based on thermodynamic calculations using our determined data about possible mechanochemical metathesis

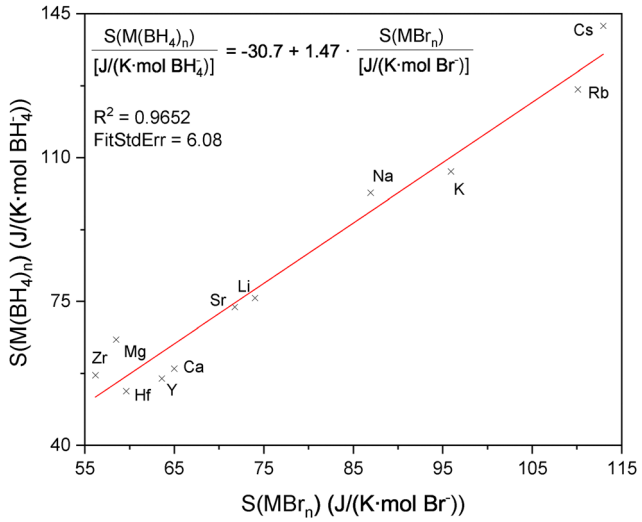

Fig. 7 Linear correlation between the absolute entropies of metal boranates and the ones of the corresponding metal bromides. The fit coefficients and the standard fit error corresponding to the linear fit function can be found in the diagram as well as in Table 6.

Table 7 Results of thermodynamic calculations regarding the synthesis of $Ba(BH_4)_2$ based on mechanochemical metathesis reactions according to reaction eqn (1)

Boranate	Barium halide	Product halide	$\Delta_R G$(298.15 K) (kJ mol^{-1})
$LiBH_4$	BaF_2	LiF	−46.9
$NaBH_4$		NaF	36.2
$LiBH_4$	$BaCl_2$	LiCl	10.9
$NaBH_4$		NaCl	9.2
$LiBH_4$	$BaBr_2$	LiBr	26.3
$NaBH_4$		NaBr	10.3
$LiBH_4$	BaI_2	LiI	32.8
$NaBH_4$		NaI	2.7

reactions to produce $Ba(BH_4)_2$. All calculated reactions are based on reaction eqn (1), but taking into account $NaBH_4$ as well as BaF_2, $BaCl_2$ and $BaBr_2$ in addition to $LiBH_4$ and BaI_2. The Gibbs free energies of reaction are shown in Table 7.

From a thermodynamic point of view, the mechanochemical synthesis of $Ba(BH_4)_2$ is only possible using BaF_2 and $LiBH_4$ as reactants as indicated by the negative Gibbs free energy of reaction. For this situation the main driver is the high stability of the product LiF.[55] However, taking into account the uncertainty of the enthalpy of formation value of $Ba(BH_4)_2$, a synthesis using $NaBH_4$ and BaI_2 as reactants in a mechanochemical metathesis seems likely, too. In addition, the literature states a possible wet chemical synthesis using $LiBH_4$ and BaI_2.[39] Therefore, it seems likely, that $Ba(BH_4)_2$ can be produced from a mixture of BaI_2 and $NaBH_4$ in the liquid phase.

Calculations regarding the decomposition behaviour and rehydrogenation capability

Eqn (16) was used for the calculations of the equilibrium hydrogen pressure of $Ba(BH_4)_2$ resulting from the reaction eqn (2) and (3). The reaction between BaH_2 and B (see reaction eqn (17)) was also studied because it may occur as an intermediate step during the decomposition of $Ba(BH_4)_2$ into BaB_6, BaH_2 and hydrogen (reaction eqn (3)).

$$p_{eq} = p^{\circ} \cdot e^{-\frac{\Delta_{dec}G^{\circ}(T)}{R \cdot T \cdot \sum_i \nu_{i,gas}}} \quad (16)$$

$$\frac{1}{3}BaH_2 + 2B \rightarrow \frac{1}{3}BaB_6 + \frac{1}{3}H_2 \quad (17)$$

The calculation of other decomposition reactions was not performed, because no thermodynamic data for complex intermediates, such as BaB_xH_y, are currently available to our knowledge.

The temperature dependence of the Gibbs free energy change for the discussed decomposition reactions is shown in Fig. 8.

The diagram in Fig. 8 exhibits a favoured decomposition according to reaction eqn (3) from a thermodynamic point of view. The decomposition into a hexaboride instead of elemental boron has been found for $Sr(BH_4)_2$, too.[26] In contrast, β-$Ca(BH_4)_2$ decomposes into CaH_2, B and hydrogen.[24,58] However, $Y(BH_4)_3$[25] as well as $Zr(BH_4)_4$ and $Hf(BH_4)_4$[23] decompose into a metal hydride and boron and, at high temperatures, subsequently into metal borides under a further release of hydrogen. The difference between the described decomposition behaviour can be attributed to the differences in the thermodynamic stability of the metal borides as solid decomposition products as well as kinetic hindrances due to the increased decomposition temperatures of $Sr(BH_4)_2$ and $Ba(BH_4)_2$ compared to the other mentioned boranates.[8,58]

The calculated decomposition temperature for the reaction eqn (3) is about (250 ± 20) °C at a pressure of 1 bar, which is much lower than the experimental ones reported in the literature (higher than 385 °C, the decomposition is accompanied by the melting of the compound[37]). The difference between the calculated and the experimental determined decomposition temperature is typical for boranates. However, there is a simple explanation for this effect: kinetic constraints in the decomposition process can contribute to increased decomposition temperatures, as this is a common phenomenon of this class of compounds.[23,24,58]

Fig. 9 demonstrates the thermal stability of the favoured decomposition reaction eqn (3) of $Ba(BH_4)_2$ in comparison to other boranates.[8,40] Furthermore, a rehydrogenation of the thermodynamically favoured solid decomposition products BaH_2 and BaB_6 to $Ba(BH_4)_2$ can only be achieved, if it takes place directly *via* the reverse reaction of reaction eqn (3) instead *via* an intermediate step forming BaH_2 and B (reverse reaction of reaction eqn (17)). The formation of the intermediates BaH_2 and B is not possible from a thermodynamic point of view, since the Gibbs free energy of reaction stays positive for the reverse reaction of reaction eqn (17) over the entire temperature range. This fact can also be traced back for reaction eqn (17) for which the enthalpy of reaction is positive at relevant pressures, which is also a sign for an irreversible reaction.

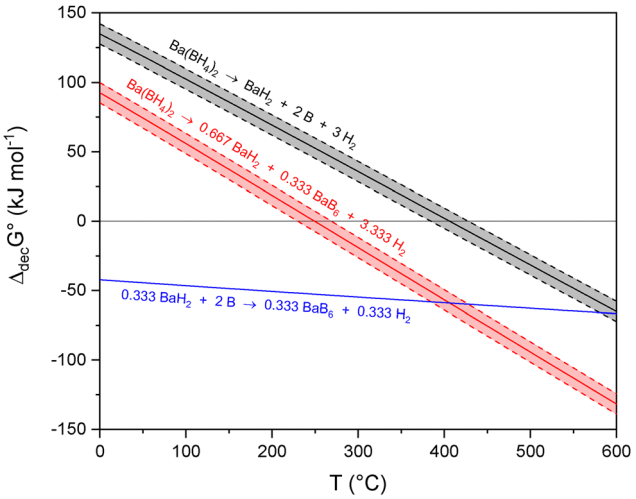

Fig. 8 Gibbs free energy of decomposition for reaction eqn (2), reaction eqn (3) and reaction eqn (17) at a pressure of 1 bar. All calculations are performed taking into account the uncertainty of the enthalpy of formation value of $Ba(BH_4)_2$.

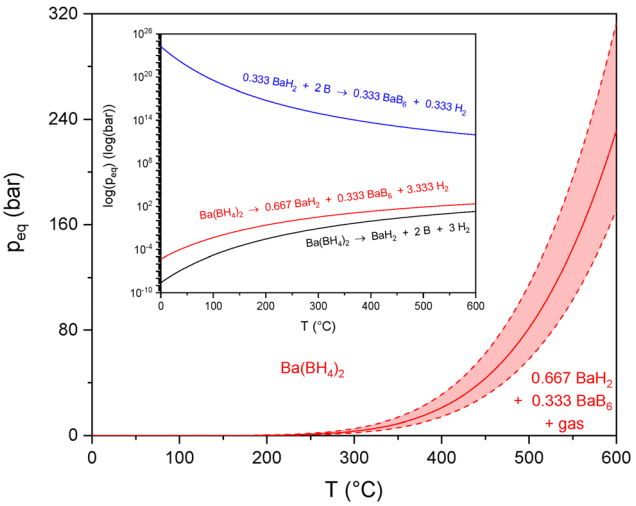

Fig. 9 Equilibrium hydrogen pressure of $Ba(BH_4)_2$ *versus* temperature calculated from eqn (16) according to reaction eqn (3). The insert displays the data equilibrium hydrogen pressures on a logarithmic scale for reaction eqn (2), reaction eqn (3) and reaction eqn (17). All calculations are performed taking into account the uncertainty of the enthalpy of formation value of $Ba(BH_4)_2$.

Conclusions

The heat capacity function and absolute entropy of o1-$Ba(BH_4)_2$ was calculated over a broad temperature range employing DFT and statistical thermodynamics based on the orthorhombic room temperature structure. The absolute entropy was determined to be $S(298.15\ \mathrm{K}) = 144.3\ \mathrm{J\ mol^{-1}\ K^{-1}}$. Using three different correlation procedures, we obtained a mean value for the enthalpy of formation of $\Delta_F H(298.15\ \mathrm{K}) = (-413.0 \pm 7.3)\ \mathrm{kJ\ mol^{-1}}$ based on the respective values of metal perchlorates and bromides as well as the electronegativity according to Pauling of the corresponding metals.

Of the three correlation procedures, the bromide correlation was based on the largest number of literature values and thus should display the smallest uncertainties of the fitting coefficients assuming a comparable quality of the input data. Therefore, it can also be assumed that it deliver the most reliable data. In addition, it was shown that in contrast to the correlation based on the Pauling electronegativity the bromide one can be applied to an extended group of boranates (the ones possessing a higher degree of covalent bonding).

The two possible decomposition reactions of $Ba(BH_4)_2$ known from literature were discussed in the light of thermodynamics using data derived from correlation functions and DFT calculations. The results from this analysis favour the interpretation that the decomposition occurs similarly to the one of $Sr(BH_4)_2$, *i.e.* forming a stable metal boride (BaB_6) and the metal dihydride as well as hydrogen. The analysis also shows that the rehydrogenation can thermodynamically not occur *via* the reverse reaction eqn (17) but needs to proceed directly from BaB_6 to $Ba(BH_4)_2$. Regarding the similar decomposition of $Sr(BH_4)_2$ to the hexaboride allows to conclude that both materials possess equivalent rehydrogenation pathways.

Since the synthesis of $Ba(BH_4)_2$ by both solvent-mediated and mechanochemical metathesis has not been successful so far, alternative reactant combinations were explored from the thermodynamic point of view from which the combination of $LiBH_4$ and BaF_2 appears to be the most promising one.

The decomposition temperature of $Ba(BH_4)_2$ is too high for a technically relevant application. However, it is a promising candidate for the design of reactive hydride mixtures in the context of thermodynamic tuning. The barium boranate data provided enlarges the relevant data base and thus supports the characterisation of such hydride systems. Given the theoretical nature of the analysis, the next step should be the attempts of the synthesis of $Ba(BH_4)_2$ based on the calculated reactant combination suggestions followed by a comprehensive calorimetric characterisation to determine the decomposition temperature and corresponding enthalpy as well as the enthalpy of formation.

Author contributions

K. Burkmann – methodology, investigation, formal analysis, validation, visualisation, writing – original draft. M. Mehlhorn – formal analysis, visualisation, validation, data curation, writing – original draft. A. Demmer – validation, writing – review & editing. J. Kraus – formal analysis, validation, writing – review & editing. F. Habermann – validation, writing – review & editing. J. Seidel – validation, writing – review & editing. K. Bohmhammel – investigation, validation, writing – review & editing. J. Kortus – resources, writing – review & editing. F. Mertens – conceptualisation, project administration, funding acquisition, resources, supervision, writing – review & editing.

Conflicts of interest

There are no conflicts to declare.

Data availability

The data supporting this article have been included as part of the manuscript. In detail, Tables 1–3 show all values used within the following analysis. The data to calculate the $G(T)$ values and derived quantities are available on GitHub (**https://github.com/MarkusMehlhorn/Ba-BH4-2-Thermodynamics.git**).

Acknowledgements

The reported research activities have been financially supported from the Deutsche Forschungsgemeinschaft (DFG project ID 449160425). K. Burkmann received financial support from the Free State of Saxony (Landesstipendium zur Graduiertenförderung). The authors would like to thank Dr. Lesia Sandig-Predzymirksa for the translation of several Russian original language papers.

Notes and references

1 E. Callini, Z. Ö. K. Atakli, B. C. Hauback, S.-I. Orimo, C. Jensen, M. Dornheim, D. Grant, Y. W. Cho, P. Chen, B. Hjörvarsson, P. de Jongh, C. Weidenthaler, M. Baricco, M. Paskevicius, T. R. Jensen, M. E. Bowden, T. S. Autrey and A. Züttel, *Appl. Phys. A: Mater. Sci. Process.*, 2016, **122**, 353–375.
2 M. Paskevicius, L. H. Jepsen, P. Schouwink, R. Černý, D. B. Ravnsbæk, Y. Filinchuk, M. Dornheim, F. Besenbacher and T. R. Jensen, *Chem. Soc. Rev.*, 2017, **46**, 1565–1634.
3 B. Richter, J. B. Grinderslev, K. T. Møller, M. Paskevicius and T. R. Jensen, *Inorg. Chem.*, 2018, **57**, 10768–10780.
4 C. Milanese, T. R. Jensen, B. C. Hauback, C. Pistidda, M. Dornheim, H. Yang, L. Lombardo, A. Zuettel, Y. Filinchuk, P. Ngene, P. E. de Jongh, C. E. Buckley, E. M. Dematteis and M. Baricco, *Int. J. Hydrogen Energy*, 2019, **44**, 7860–7874.
5 K. Suárez-Alcántara, J. R. Tena-Garcia and R. Guerrero-Ortiz, *Materials*, 2019, **12**, 2724–2787.
6 J. B. Grinderslev, K. T. Møller, M. Bremholm and T. R. Jensen, *Inorg. Chem.*, 2019, **58**, 5503–5517.
7 F. Marques, M. Balcerzak, F. Winkelmann, G. Zepon and M. Felderhoff, *Energy Environ. Sci.*, 2021, **14**, 5191–5227.
8 K. Suárez-Alcántara and J. R. Tena García, *Materials*, 2021, **14**, 2561.
9 R. Černý, F. Murgia and M. Brighi, *J. Alloys Compd.*, 2022, **895**, 162659.
10 E. M. Dematteis, M. B. Amdisen, T. Autrey, J. Barale, M. E. Bowden, C. E. Buckley, Y. W. Cho, S. Deledda, M. Dornheim, P. de Jongh, J. B. Grinderslev, G. Gizer, V. Gulino, B. C. Hauback, M. Heere, T. W. Heo, T. D. Humphries, T. R. Jensen, S. Y. Kang, Y.-S. Lee, H.-W. Li, S. Li, K. T. Møller, P. Ngene, S.-I. Orimo, M. Paskevicius, M. Polanski, S. Takagi, L. Wan, B. C. Wood, M. Hirscher and M. Baricco, *Prog. Energy*, 2022, **4**, 032009.
11 C. Comanescu, *Materials*, 2022, **15**, 2286.
12 N. Klopčič, I. Grimmer, F. Winkler, M. Sartory and A. Trattner, *J. Energy Storage*, 2023, **72**, 108456.
13 M. Palumbo, E. M. Dematteis, L. Fenocchio, G. Cacciamani and M. Baricco, *J. Phase Equilib. Diffus.*, 2024, **45**, 273–289.
14 Z. Cao, F. Habermann, K. Burkmann, M. Felderhoff and F. Mertens, *Hydrogen*, 2024, **5**, 241–279.
15 M. Baricco, E. M. Dematteis, J. Barale, M. Costamagna, M. F. Sgroi, M. Palumbo and P. Rizzi, *Pure Appl. Chem.*, 2024, **96**, 511–524.
16 C. Drawer, J. Lange and M. Kaltschmitt, *J. Energy Storage*, 2024, **77**, 109988.
17 L. H. Jepsen, M. B. Ley, R. Černý, Y.-S. Lee, Y. W. Cho, D. Ravnsbæk, F. Besenbacher, J. Skibsted and T. R. Jensen, *Inorg. Chem.*, 2015, **54**, 7402–7414.
18 J. Ortmeyer, A. Bodach, L. Sandig-Predzymirska, B. Zibrowius, F. Mertens and M. Felderhoff, *ChemPhysChem*, 2019, **20**, 1360–1368.
19 L. Sandig-Predzymirska, J. Ortmeyer, J. Wagler, E. Brendler, F. Habermann, M. Anders, M. Felderhoff and F. Mertens, *Dalton Trans.*, 2020, **49**, 17689–17698.
20 J. B. Grinderslev, M. B. Amdisen and T. R. Jensen, *Inorganics*, 2020, **8**, 57.
21 E. M. Dematteis, S. R. Jensen, T. R. Jensen and M. Baricco, *J. Chem. Thermodyn.*, 2020, **143**, 106055.
22 E. R. Pinatel, E. Albanese, B. Civalleri and M. Baricco, *J. Alloys Compd.*, 2015, **645**, S64–S68.
23 K. Burkmann, F. Habermann, E. Schumann, J. Kraus, B. Störr, H. Schmidt, E. Brendler, J. Seidel, K. Bohmhammel, J. Kortus and F. Mertens, *New J. Chem.*, 2024, **48**, 2743–2754.
24 K. Burkmann, F. Habermann, A. Walnsch, B. Störr, J. Seidel, K. Bohmhammel, R. Gumeniuk and F. Mertens, *submitted to ChemPhysChem*, 2025.
25 K. Burkmann, F. Habermann, B. Störr, J. Seidel, R. Gumeniuk, K. Bohmhammel and F. Mertens, *RSC Mechanochem.*, 2025, **2**, 563–572.
26 K. Burkmann, A. Demmer, F. Habermann, B. Hansel, B. Störr, J. Seidel, R. Gumeniuk, M. Bertau, K. Bohmhammel and F. Mertens, *J. Therm. Anal. Calorim.*, 2025, **150**, 5409–5417.
27 F. Habermann, K. Burkmann, B. Hansel, B. Störr, C. Schimpf, J. Seidel, M. Bertau and F. Mertens, *Dalton Trans.*, 2023, **52**, 4880–4890.
28 F. Habermann, A. Wirth, K. Burkmann, B. Störr, J. Seidel, R. Gumeniuk, K. Bohmhammel and F. Mertens, *ChemPhysChem*, 2024, **25**, e202300748.
29 F. Habermann, K. Burkmann, J. Kraus, B. Störr, J. Seidel, K. Bohmhammel, J. Kortus, R. Gumeniuk and F. Mertens, *J. Alloys Compd.*, 2024, **980**, 173476.
30 F. Habermann, A. Wirth, K. Burkmann, J. Kraus, B. Störr, H. Stöcker, J. Seidel, J. Kortus, D. C. Meyer, R. Gumeniuk, K. Bohmhammel and F. Mertens, *RSC Mechanochem.*, 2025, **2**, 603–615.
31 J. J. Vajo, F. Mertens, C. C. Ahn, R. C. Bowman and B. Fultz, *J. Phys. Chem. B*, 2004, **108**, 13977–13983.
32 J. J. Vajo, S. L. Skeith and F. Mertens, *J. Phys. Chem. B*, 2005, **109**, 3719–3722.

33 E. Wiberg and R. Hartwimmer, *Z. Naturforsch. B*, 1955, **10**, 294–295.
34 E. Wiberg, H. Nöth and R. Hartwimmer, *Z. Naturforsch. B*, 1955, **10**, 292–294.
35 E. Wiberg and R. Hartwimmer, *Z. Naturforsch. B*, 1955, **10**, 295–296.
36 M. Sharma, E. Didelot, A. Spyratou, L. M. Lawson Daku, R. Černý and H. Hagemann, *Inorg. Chem.*, 2016, **55**, 7090–7097.
37 V. I. Mikheeva, L. N. Tolmacheva and A. S. Sizareva, *Russ. J. Inorg. Chem.*, 1974, **19**, 622–623.
38 H. C. Brown, Y. M. Choi and S. Narasimhan, *Inorg. Chem.*, 1982, **21**, 3657–3661.
39 V. I. Mikheeva and L. N. Tolmacheva, *Russ. J. Inorg. Chem.*, 1974, **19**, 665–666.
40 V. N. Konoplev, N. N. Mal'tseva and V. S. Khain, *Koord. Khim.*, 1992, **18**, 1143–1166.
41 A. Demmer, *Bachelorarbeit*, TU Bergakademie Freiberg, Freiberg, 2023.
42 R. P. Stoffel, C. Wessel, M.-W. Lumey and R. Dronskowski, *Angew. Chem.*, 2010, **122**, 5370–5395.
43 P. Giannozzi, S. Baroni, N. Bonini, M. Calandra, R. Car, C. Cavazzoni, D. Ceresoli, G. L. Chiarotti, M. Cococcioni, I. Dabo, A. D. Corso, S. de Gironcoli, S. Fabris, G. Fratesi, R. Gebauer, U. Gerstmann, C. Gougoussis, A. Kokalj, M. Lazzeri, L. Martin-Samos, N. Marzari, F. Mauri, R. Mazzarello, S. Paolini, A. Pasquarello, L. Paulatto, C. Sbraccia, S. Scandolo, G. Sclauzero, A. P. Seitsonen, A. Smogunov, P. Umari and R. M. Wentzcovitch, *J. Phys.: Condens. Matter*, 2009, **21**, 395502-1–395502-19.
44 P. Giannozzi, O. Andreussi, T. Brumme, O. Bunau, M. Boungiorno Nardelli, M. Calandra, R. Car, C. Cavazzoni, D. Ceresoli, M. Cococcioni, N. Colonna, I. Carnimeo, A. D. Corso, S. de Gironcoli, P. Delugas, R. A. DiStasio Jr, A. Ferretti, A. Floris, G. Fratesi, G. Fugallo, R. Gebauer, U. Gerstmann, F. Giustino, T. Gorni, J. Jia, M. Kawamura, H.-Y. Ko, A. Kokalj, E. Kücükbenli, M. Lazzeri, M. Marsili, N. Marzari, F. Mauri, N. L. Nguyen, H.-V. Nguyen, A. Otera-de-la Roza, L. Paulatto, S. Poncé, D. Rocca, R. Sabatini, B. Santra, M. Schlipf, A. P. Seitsonen, A. Smogunov, I. Timrov, T. Thonhauser, P. Umari, N. Vast, X. Wu and S. Baroni, *J. Phys.: Condens. Matter*, 2017, **29**, 465901-1–465901-30.
45 P. Giannozzi, O. Baseggio, P. Bonfà, D. Brunato, R. Car, I. Carnimeo, C. Cavazzoni, S. de Gironcoli, P. Delugas, F. F. Ruffino, A. Ferretti, N. Marzari, I. Timrov, A. Urru and S. Baroni, *J. Chem. Phys.*, 2020, **152**, 154105-1–154105-11.
46 J. P. Perdew, K. Burke and M. Ernzerhof, *Phys. Rev. Lett.*, 1996, **77**, 3865–3868.
47 G. Prandini, A. Marrazzo, I. E. Castelli, N. Mounet and N. Marzari, A Standard Solid State Pseudopotentials (SSSP) library optimized for precision and efficiency (Version 1.1, data download).
48 S. Schmerler, *elcorto/pwtools*, 2021, **https://zenodo.org/records/13128303**.
49 Y. Nakamori, K. Miwa, A. Ninomiya, H. Li, N. Ohba, S.-I. Towata, A. Züttel and S.-I. Orimo, *Phys. Rev. B:Condens. Matter Mater. Phys.*, 2006, **74**, 045126.
50 K. Miwa, N. Ohba, S.-I. Towata, Y. Nakamori, A. Züttel and S.-I. Orimo, *J. Alloys Compd.*, 2007, **446–447**, 310–314.
51 V. A. Kuznetsov and T. N. Dymova, *Russ. Chem. Bull.*, 1971, **20**, 204–208.
52 M. K. Karapet'yants, *Russ. J. Inorg. Chem.*, 1965, **10**, 837–841.
53 F. Habermann, PhD dissertation, TU Bergakademie Freiberg, Freiberg, 2024.
54 H. Hagemann, *ChemistrySelect*, 2019, **4**, 8989–8992.
55 A. Roine, *HSC Chemistry*, 2002, **https://www.hsc-chemistry.com/**.
56 *CRC handbook of chemistry and physics: A ready-reference book of chemical and physical data*, ed. J. R. Rumble and T. J. Bruno, CRC Press, Boca Raton, Florida, 2020th edn, 2020.
57 S. H. Lee, V. R. Manga and Z.-K. Liu, *Int. J. Hydrogen Energy*, 2010, **35**, 6812–6821.
58 K. Burkmann, PhD dissertation, TU Bergakademie Freiberg, Freiberg, 2024.
59 W. Xiang-Yun, J. T. Zhu, J. Goudiakas and J. Fuger, *J. Chem. Thermodyn.*, 1988, **20**, 1195–1202.
60 A. Kurbonbekov, T. H. Alikhanova, A. Badalov and V. K. Marufi, *Dokl. Akad. Nauk SSSR*, 1990, **33**, 393–395.
61 V. E. Gorbunov, K. S. Gavrichev and V. B. Lazarev, *Russ. J. Inorg. Chem.*, 1986, **60**, 1240–1242.
62 K. Burkmann, F. Habermann, R. Gumeniuk and F. Mertens, *Z. Naturforsch. B*, 2024, **79**, 293–296.
63 C. G. Maier and K. K. Kelley, *J. Am. Chem. Soc.*, 1932, **54**, 3243–3246.
64 S. Shang, T. Wang and Z.-K. Liu, *CALPHAD:Comput. Coupling Phase Diagrams Thermochem.*, 2007, **31**, 286–291.
65 G. Bergerhoff and I. D. Brown, *Crystallographic Databases*, International Union of Crystallography, Chester, 1987.
66 S. Baroni, P. Giannozzi and A. Testa, *Phys. Rev. Lett.*, 1987, **59**, 2662–2665.
67 S. Y. Savrasov, *Phys. Rev. B:Condens. Matter Mater. Phys.*, 1996, **54**, 16470–16486.
68 X. Gonze and C. Lee, *Phys. Rev. B:Condens. Matter Mater. Phys.*, 1997, **55**, 10355–10368.
69 K. Miwa, M. Aoki, T. Noritake, N. Ohba, Y. Nakamori, S.-I. Towata, A. Züttel and S.-I. Orimo, *Phys. Rev. B:Condens. Matter Mater. Phys.*, 2006, **74**, 155122.
70 Y.-S. Lee, J.-H. Shim and Y. W. Cho, *J. Phys. Chem. C*, 2010, **114**, 12833–12837.
71 T. Sato, K. Miwa, Y. Nakamori, K. Ohoyama, H.-W. Li, T. Noritake, M. Aoki, S.-I. Towata and S.-I. Orimo, *Phys. Rev. B:Condens. Matter Mater. Phys.*, 2008, **77**, 104114.
72 C. Wolverton and V. Ozoliņš, *Phys. Rev. B:Condens. Matter Mater. Phys.*, 2007, **75**, 064101-1–064101-15.
73 S. Baroni, P. Giannozzi and E. Isaev, *Rev. Mineral. Geochem.*, 2010, **71**, 39–57.
74 H. L. Lukas, S. G. Fries and B. Sundman, *Computational thermodynamics: The Calphad method*, Cambridge Univ. Press, Cambridge, 2007.
75 M. Otto, *Chemometrics*, Wiley, 3rd edn, 2016.
76 *Evaluation of measurement data – Guide to the expression of uncertainty in measurement*, ed. Joint Committee for Guides in Metrology, 1st edn, 2008.

